

# Cluster Phase Chemistry: Collisions of Vibrationally Excited Cationic Dicarboxylic Acid Clusters with Water Molecules Initiate Dissociation of Cluster Components

Hugh I. Kim and J. L. Beauchamp\*

Noyes Laboratory of Chemical Physics, California Institute of Technology, Pasadena, California 91125

Received: January 25, 2007; In Final Form: April 12, 2007

A homologous series of cationic gas-phase clusters of dicarboxylic acids (oxalic acid, malonic acid, succinic acid, glutaric acid, and adipic acid) generated via electrospray ionization (ESI) are investigated using collision-induced dissociation (CID). Singly charged cationic clusters with the composition  $(\text{Na}^+)_{2n+1}(\text{dicarboxylate}^{2-})_n$ , where  $n = 1-5$ , are observed as major gas-phase species. Significant abundances of singly charged sodiated hydrogen dicarboxylate clusters with the composition  $(\text{Na}^+)_{2n}(\text{dicarboxylate}^{2-})_n(\text{H}^+)$ , where  $n = 1-6$ , are observed with oxalic acid, malonic acid, and succinic acid. Isolation of the clusters followed by CID results mainly in sequential loss of disodium dicarboxylate moieties for the clusters of succinic acid, glutaric acid, and adipic acid. However, the dimer of sodiated hydrogen succinate, all malonate clusters, and all oxalate clusters, with the exception of the dimer, exhibit complex chemical reactions initiated by the collision of vibrationally excited clusters with water molecules. Generally, water molecules serve as proton donors for reacting dicarboxylate anions in the cluster, initiating dissociation pathways such as the decomposition of the malonate ion to yield an acetate ion and  $\text{CO}_2$ . The reactivity of several mixed dicarboxylate clusters is also reported. For example, malonate anion is shown to be more reactive than oxalate anion for decarboxylation when both are present in a cluster. The energetics of several representative cluster phase reactions are evaluated using computational modeling. The present results for cationic clusters are compared and contrasted to earlier studies of anionic sodiated dicarboxylic acid clusters.

## 1. Introduction

Molecular clusters provide unique model systems for structure and reactivity studies, bridging the gap between the gas phase and bulk phase. Ionic clusters are a rich source of interesting chemical reactions that can be promoted by collisional activation and bimolecular collisions. Recent reports from our laboratory have focused on studies of chemical reactions that occur between cluster components, other than simple dissociations, following collisional activation. For example, previous studies have demonstrated the synthesis of ATP from clusters of the AMP sodium salt,<sup>1</sup> as well as  $\text{S}_{\text{N}}2$  and E2 reactions of tetraalkylammonium ions with triphosphate and DNA anions.<sup>2</sup> Further, we have reported phosphorylation of alcohols via cluster phase reactions of triphosphate and molecules possessing hydroxyl functional groups.<sup>3</sup> More recently, we have shown that bimolecular collisions of collisionally activated clusters with small molecules can introduce energetically favorable pathways for reactions of cluster components.<sup>4</sup> For example, while collisionally activated singly charged proton-free anionic clusters of succinic acid (C4), glutaric acid (C5), and adipic acid (C6) generally exhibit sequential loss of disodium dicarboxylate moieties, all oxalic acid (C2) and malonic acid (C3) clusters and dimers of C4 and C5 exhibit more complex chemical reactions which result from collisions with water molecules. Water molecules donate protons to dicarboxylate anions, initiating chemical processes that include decarboxylation of the diacid anion.

Dicarboxylic acids are ubiquitous in the environment. They are important metabolic and oxidative end products of complex natural products.<sup>5</sup> Dicarboxylic acids are known to be significant

contributors of organic mass in atmospheric aerosols.<sup>6-9</sup> They contribute to the acidity of precipitation and act as nuclei for cloud formation in the marine atmospheric environment.<sup>6</sup> Their high water affinities and low vapor pressure allow dicarboxylic acids to accumulate in aerosols.<sup>10,11</sup> Gas-phase dicarboxylic acids can aggregate with sodium cation, which is a major component of sea salt particles in the atmosphere,<sup>12,13</sup> forming sodium-dicarboxylic acid clusters, which are the subject of this investigation.

In the present paper, a homologous series of cationic gas-phase clusters of dicarboxylic acids (oxalic acid, malonic acid, succinic acid, glutaric acid, and adipic acid) generated via electrospray ionization (ESI) are investigated using collision-induced dissociation (CID). Singly charged cationic clusters with the composition  $(\text{Na}^+)_{2n+1}(\text{dicarboxylate}^{2-})_n$ , where  $n = 1-5$ , are observed as major gas-phase species. Significant abundances of singly charged sodiated hydrogen dicarboxylate clusters with the composition  $(\text{Na}^+)_{2n}(\text{dicarboxylate}^{2-})_n(\text{H}^+)$ , where  $n = 1-6$ , are observed with oxalic acid, malonic acid, and succinic acid (C2–C4). This study focuses on the observation that all oxalate (C2) clusters larger than the dimer, malonate (C3) clusters, and the dimer of sodiated hydrogen succinate (C4) exhibit complex chemical reactions initiated by the collision of water molecules and collisionally activated clusters. This is in contrast to the behavior of the larger acids, where sequential loss of disodium dicarboxylate moieties results from CID of succinic acid, glutaric acid, and adipic acid (C4–C6) clusters. Generally, water molecules serve as proton donors for reacting dicarboxylate anions in the cluster, initiating dissociation pathways such as the decomposition of the malonate ion to yield an acetate ion and  $\text{CO}_2$ . We present results comparing the reactivity of different

\* To whom correspondence should be addressed. E-mail: jlbchamp@caltech.edu.

**TABLE 1: Occurrence of Sodiater Clusters (C) of Small Dicarboxylic Acid (C2–C6) and Cluster Phase Reactions (R) in the Present Study<sup>a</sup>**

	$(\text{Na}^+)_{2n+1}(\text{dicarboxylate}^{2-})_n$										$(\text{Na}^+)_{2n}(\text{dicarboxylate}^{2-})_n(\text{H}^+)$									
	$n=1$		$n=2$		$n=3$		$n=4$		$n=5$		$n=1$		$n=2$		$n=3$		$n=4$		$n=5$	
	C	R	C	R	C	R	C	R	C	R	C	R	C	R	C	R	C	R	C	R
C2	○	○	○	×	○	○	○	○	○	○	×	×	○	○	○	○	○	○	○	○
C3	○	○	○	○	○	○	○	○	○	○	○	×	○	○	○	○	○	○	○	○
C4	○	○	○	×	○	×	○	×	○	×	○	×	○	○	○	○	×	○	×	×
C5	○	×	○	×	○	×	○	×	○	×	×	×	×	×	×	×	×	×	×	×
C6	○	×	○	×	○	×	○	×	○	×	×	×	×	×	×	×	×	×	×	×

<sup>a</sup> The presence of the cluster and the cluster phase reaction is indicated with empty circles (○), while the absence is indicated with crosses (×).

dicarboxylate anions in several mixed clusters. For example, it is shown below that the malonate anion is more reactive than the oxalate anion for decarboxylation when both are present in a cluster. The mechanisms and energetics of the observed reactions are evaluated by means of computational modeling.

Section 2 of this study provides experimental details. Results and Discussion are combined in section 3. Sections 3.1.1–3.1.4 present and analyze data for the proton-free sodiated dicarboxylates, with emphasis on the results for the smaller members of the series of acids since they exhibit more complex and interesting reactions other than simple cluster dissociation. Experiments summarized in sections 3.2.1 and 3.2.2 consider the effect that the introduction of a proton to replace a sodium ion in the cluster has on the observed reactions. On the basis of the results presented in sections 3.1 and 3.2, we detail in section 3.3 the competitive reactivity of the smaller diacids when they appear in sodiated mixed dicarboxylate clusters. Theoretical analysis of some key processes important in describing the cluster phase chemistry of the dicarboxylic acids is presented separately in section 3.4. The conclusion in section 4 provides a concise summary of the significant observations in this study.

## 2. Experimental Section

All chemicals used for the present study (oxalic acid, malonic acid, succinic acid, glutaric acid, adipic acid, disodium oxalate, disodium malonate, disodium succinate, and sodium chloride) were purchased from Sigma Chemical Co. (St. Louis, MO) and used without further purification. All solvents (water and methanol) are HPLC grade and were purchased from J. T. Baker (Phillipsburg, NJ). For the sodium dicarboxylate studies, C2–C4 samples were prepared by dissolving disodium salts in a 50:50 methanol/water mixture solvent. C5 and C6 samples were prepared by dissolving stoichiometric amounts of sodium chloride and the dicarboxylic acid in the solvent. Total sample concentrations of C2–C4 varied over a range of 200–300  $\mu\text{M}$ , while the total sample concentration of C5 and C6 was at 100  $\mu\text{M}$ . Mixtures of C2 and C3 with other dicarboxylic acids were prepared by dissolving stoichiometric amounts of sodium chloride and dicarboxylic acids in the solvent. Total sample concentrations varied over a range of 100–200  $\mu\text{M}$ .

Experiments were performed on a Thermo Finnigan LCQ Deca ion trap mass spectrometer (ITMS) in positive mode. An electrospray voltage of 5 kV, capillary voltage of 9 V, and capillary temperature in the range of 200–300 °C are set as parameters for ESI. The pressure is estimated to be  $\sim 10^{-3}$  Torr He inside the trap. The pressure of water in the trap is estimated as  $\sim 10^{-6}$  Torr. Water vapor is considered to come from internal surface outgassing in addition to ESI solvent vapor introduced through the capillary.<sup>4</sup> Throughout the course of the present study, the operating conditions of the ESI-ITMS instrument were identical to those employed for our previous studies of anionic clusters.<sup>4</sup> Continuous isolation of the cluster ion followed by

CID (MS<sup>n</sup>) was performed until the track of the isolated ion was lost. The ESI mass spectra used in the present paper were obtained by averaging 30 scanned spectra.

Several candidate low-energy structures of the reactants and products of the observed reactions were evaluated at the PM5 level using CAChe 6.1.10 (Fujitsu, Beaverton, OR). Then, the lowest energy structures were determined using density functional theory (DFT) starting with the PM5 calculated structures. DFT calculations were performed using Jaguar 6.0 (Schrödinger, Inc., Portland, OR) utilizing the Becke three-parameter functional (B3)<sup>14</sup> combined with the correlation functional of Lee, Yang, and Parr (LYP),<sup>15</sup> using the 6-31G\*\* basis set.<sup>16</sup> Further DFT optimizations were carried out using the 6-311G\*\* basis set. The energetics and mechanisms of the observed cluster phase reactions were evaluated on the basis of the optimized structures and their corresponding energies for reactants and products.

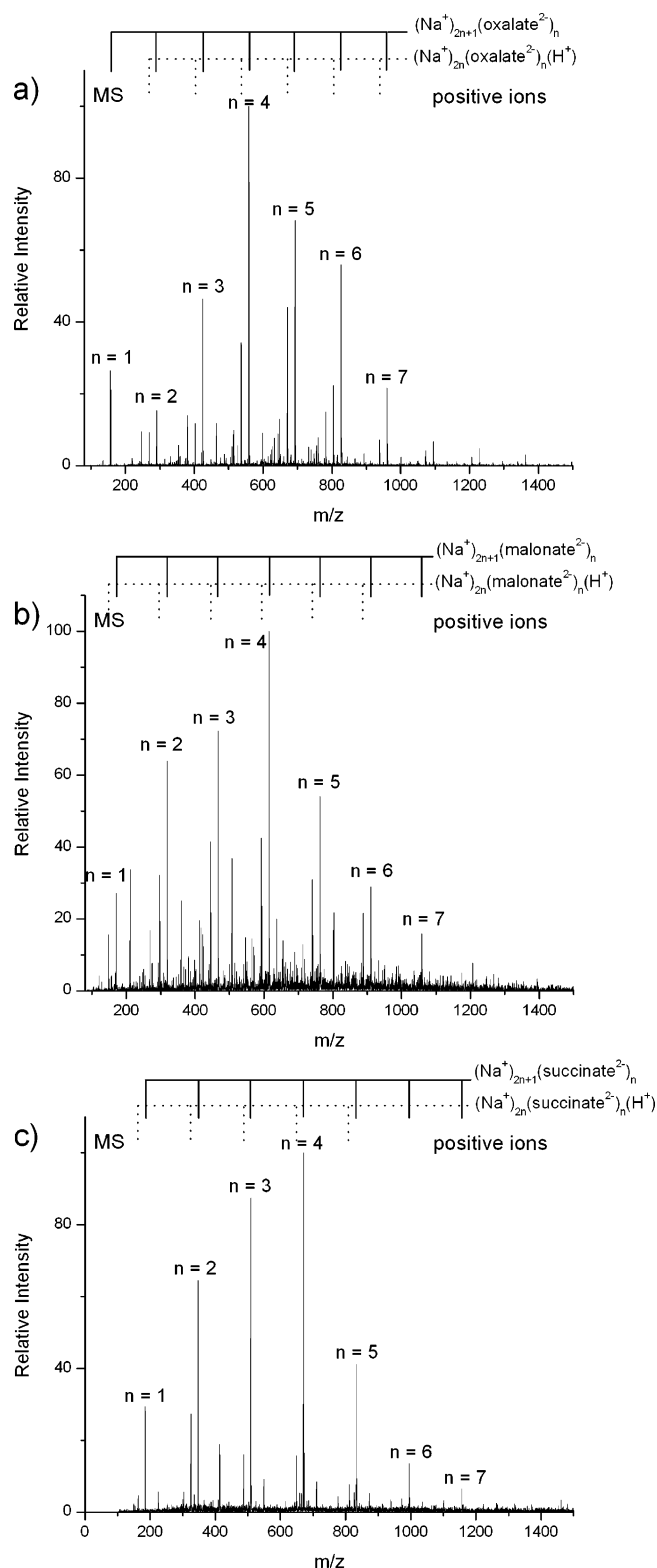
## 3. Results and Discussion

The observed clusters of small dicarboxylate cations are summarized in Table 1 along with their reactions. ESI mass spectra of C2–C4 and C5, C6 are shown in Figure 1 and Figure 2, respectively.

**3.1. Proton-Free Sodiater Dicarboxylate Clusters.** A series of proton-free sodiated dicarboxylate clusters, which are generally characterized by the composition  $(\text{Na}^+)_{2n+1}(\text{dicarboxylate}^{2-})_n$ , where  $n = 1-5$ , are observed as major gas-phase species of small dicarboxylic acid (C2–C6) in the ESI mass spectra (Figures 1 and 2). Significant abundances of singly charged sodiated hydrogen dicarboxylate clusters with the composition  $(\text{Na}^+)_{2n}(\text{dicarboxylate}^{2-})_n(\text{H}^+)$ , where  $n = 1-5$ , are observed with small dicarboxylic acids (C2–C4) along with the proton-free clusters in the spectra (Figure 1). However, no significant amount of sodiated hydrogen dicarboxylate clusters are observed with the glutaric acid (C5) and adipic acid (C6) samples (Figure 2).

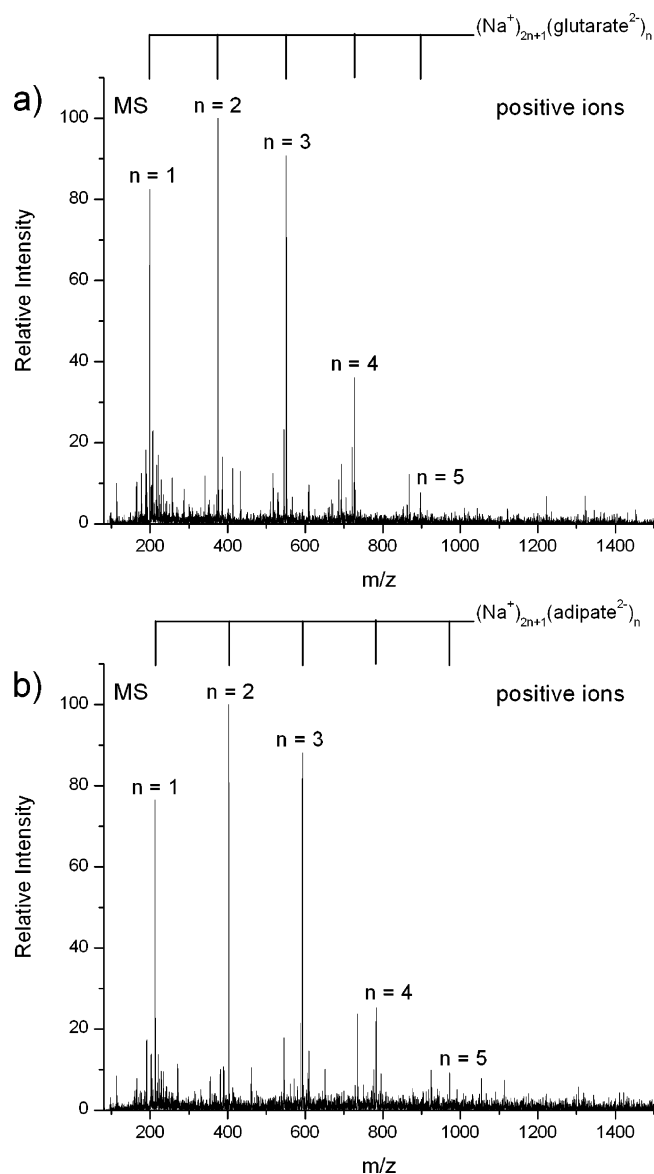
**3.1.1. Sodiater Dicarboxylate Monomers.** In contrast to anionic proton-free sodiated dicarboxylate clusters,<sup>4</sup> all of the small dicarboxylic acid (C2–C6) samples show intense peaks of monomers,  $(\text{Na}^+)_3(\text{dicarboxylate}^{2-})$ , in the mass spectra (Figures 1 and 2). The CID spectra of C2–C4 are presented in Figure 3. CID of sodiated oxalate (C2) monomer and sodiated malonate (C3) monomer yield a major product at  $m/z$  63 (Figure 3a,b). The product at  $m/z$  63 is also observed from CID of the sodiated succinate (C4) monomer with other competitive processes, yielding products at  $m/z$  141,  $m/z$  167, and  $m/z$  203 (Figure 3c). Loss of  $\text{CO}_2$  (–44 mass units) yields the product at  $m/z$  141, and the product at  $m/z$  167 results from dehydration (–18 mass units). Attachment of a water molecule (+18 mass units) yields the product at  $m/z$  203.

A common product is observed at  $m/z$  63 from the three smallest dicarboxylic acid (C2–C4) monomers. The product



**Figure 1.** ESI-MS spectra of sodiated dicarboxylate (C2–C4) clusters in positive mode. A series of proton-free sodiated dicarboxylate clusters are seen as dominant species along with a series of sodiated hydrogen oxalate clusters with (a) 300  $\mu\text{M}$  of disodium oxalate, (b) 250  $\mu\text{M}$  of disodium malonate, and (c) 200  $\mu\text{M}$  of disodium succinate.

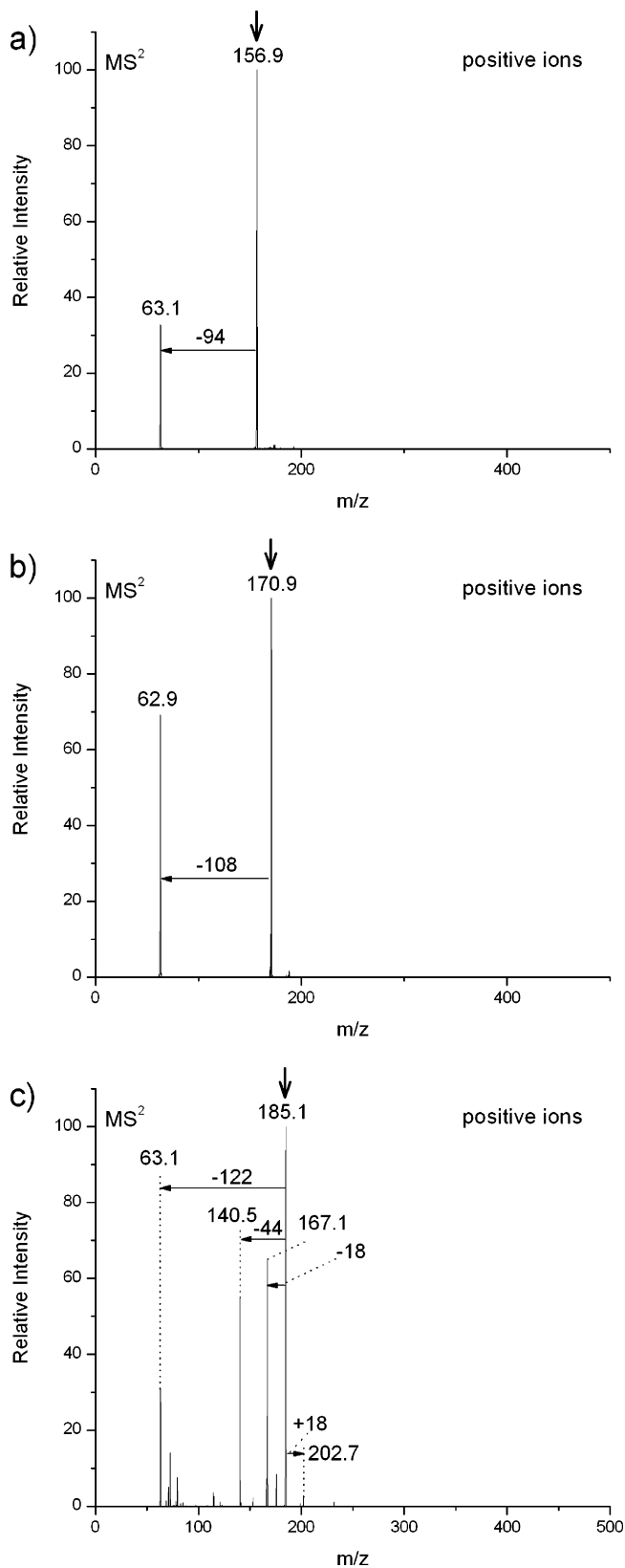
at  $m/z$  63 from C2 is yielded by the elimination of sodium hydrogen oxalate with the attachment of a H<sub>2</sub>O molecule ( $-112 + 18 = -94$  mass units). Similarly, the products at  $m/z$  63 from C3 and C4 result from the loss of sodium hydrogen malonate with H<sub>2</sub>O attachment ( $-126 + 18 = -108$  mass units) and the loss of sodium hydrogen succinate with H<sub>2</sub>O attachment ( $-140$



**Figure 2.** ESI-MS spectra of sodiated dicarboxylate (C5–C6) clusters in positive mode. A series of proton-free sodiated malonate clusters are seen as the dominant species with the mixture of 50  $\mu\text{M}$  of sodium chloride with (a) 50  $\mu\text{M}$  of glutaric acid and (b) 50  $\mu\text{M}$  of adipic acid.

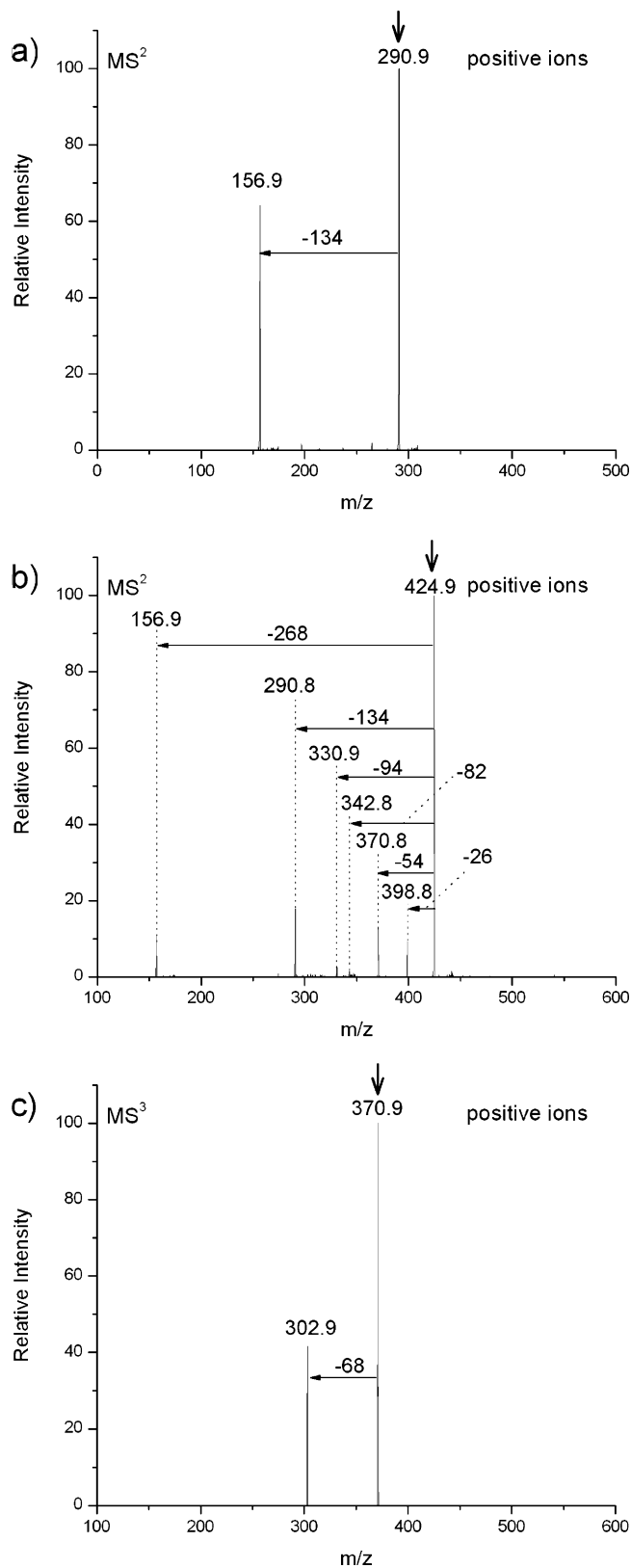
+ 18 =  $-122$  mass units), respectively. The ubiquitous product ion at  $m/z$  63 is disodium hydroxide cation, (Na<sup>+</sup>)<sub>2</sub>(<sup>-</sup>OH). On the basis of the stoichiometry of the observed products, it is inferred that the collisionally activated clusters of the three smallest proton-free sodiated dicarboxylate monomers collide with a water molecule, which donates a proton to the dicarboxylate ion concomitant with the formation of a hydroxide ion in the cluster. Using similar conditions for CID, sodiated glutarate (C5) and adipate (C6) monomers did not yield significant dissociation products.

**3.1.2. Oxalic Acid (C2).** A series of cationic proton-free sodiated oxalate clusters are found at  $m/z$  291, 425, 559, 693, 827, and 961, which correspond to  $n = 2, 3, 4, 5, 6,$  and  $7$  respectively (Figure 1a). The CID spectrum of the dimer cluster,  $n = 2$ , ( $m/z$  291) shows only monomeric dissociation, (Na<sup>+</sup>)<sub>2</sub>(oxalate<sup>2-</sup>) ( $-134$  mass units; Figure 4a). Larger clusters,  $n = 3-5$ , also show monomeric dissociations by CID. In addition to monomeric dissociations, proton-free sodiated oxalate clusters ( $n = 3-5$ ) yield four distinctive products via CID.



**Figure 3.** CID spectra of the proton-free (a) sodiated oxalate monomer, (Na<sup>+</sup>)<sub>3</sub>(oxalate<sup>2-</sup>), (b) sodiated malonate monomer, (Na<sup>+</sup>)<sub>3</sub>(malonate<sup>2-</sup>), and (c) sodiated succinate monomer, (Na<sup>+</sup>)<sub>3</sub>(succinate<sup>2-</sup>).

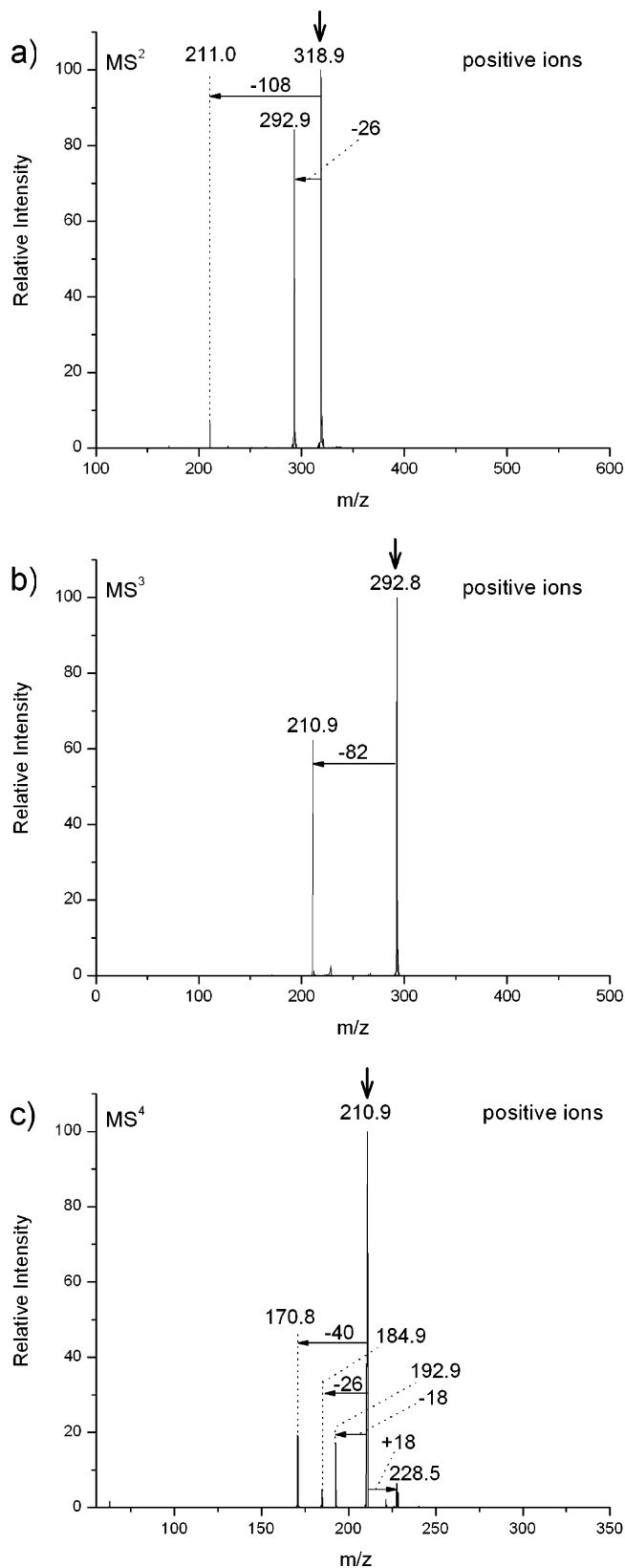
The CID spectrum of the trimer,  $n = 3$  ( $m/z$  425), is shown in Figure 4b. Other than monomeric dissociation products ( $m/z$  157 and  $m/z$  291), four distinctive products are found at  $m/z$  331, 343, 371, and 399 in the spectrum. The products at  $m/z$  331, 371, and 399 result from the loss of sodium hydrogen



**Figure 4.** (a) CID spectrum of the proton-free sodiated oxalate dimer, (Na<sup>+</sup>)<sub>5</sub>(oxalate<sup>2-</sup>)<sub>2</sub>, showing simple monomeric dissociation, (Na<sup>+</sup>)<sub>2</sub>(oxalate<sup>2-</sup>). (b) CID spectrum of the proton-free sodiated oxalate cluster, (Na<sup>+</sup>)<sub>7</sub>(oxalate<sup>2-</sup>)<sub>3</sub>, showing six distinct products. (c) MS<sup>3</sup> spectrum of the product in b at  $m/z$  371 showing exclusively loss of sodium formate, HCO<sub>2</sub>Na.

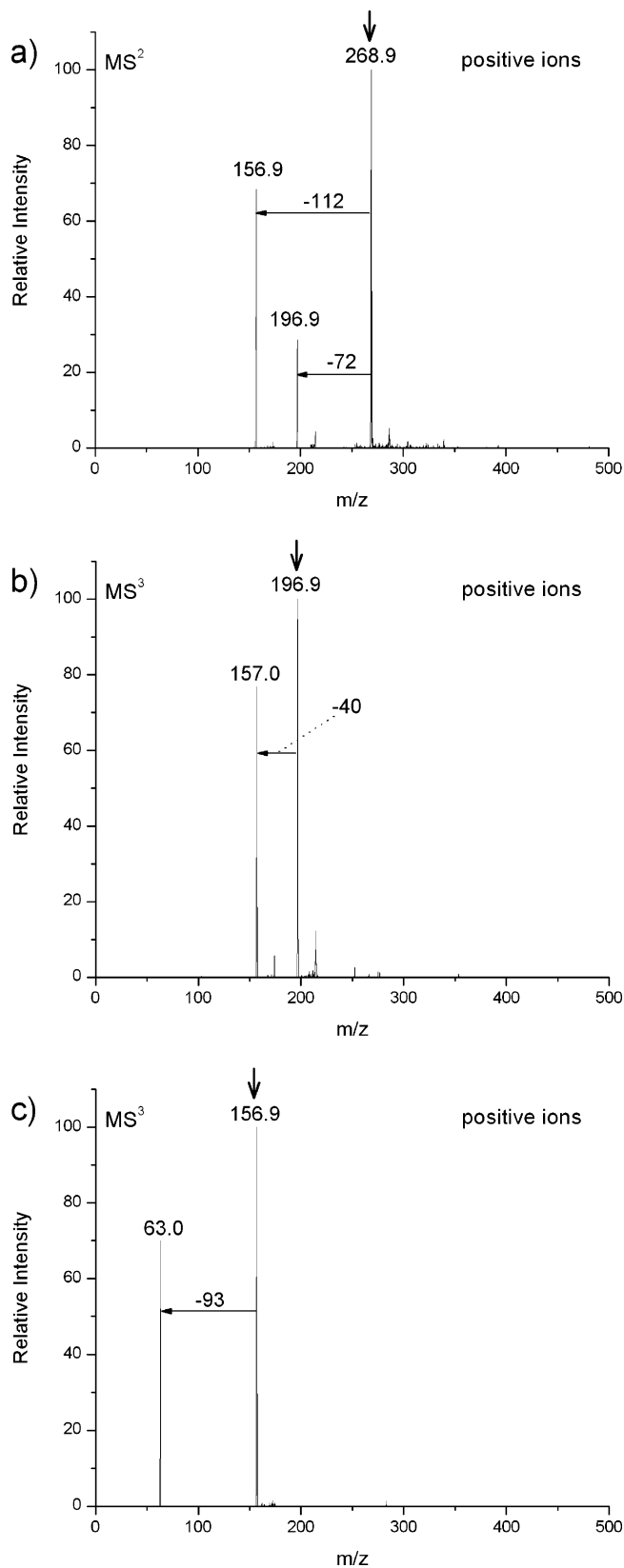
oxalate (HC<sub>2</sub>O<sub>4</sub>Na; 112 mass units) with attachment of a water molecule ( $-112 + 18 = -94$  mass units), the loss of neutral oxalic acid with attachment of two water molecules ( $-90 +$





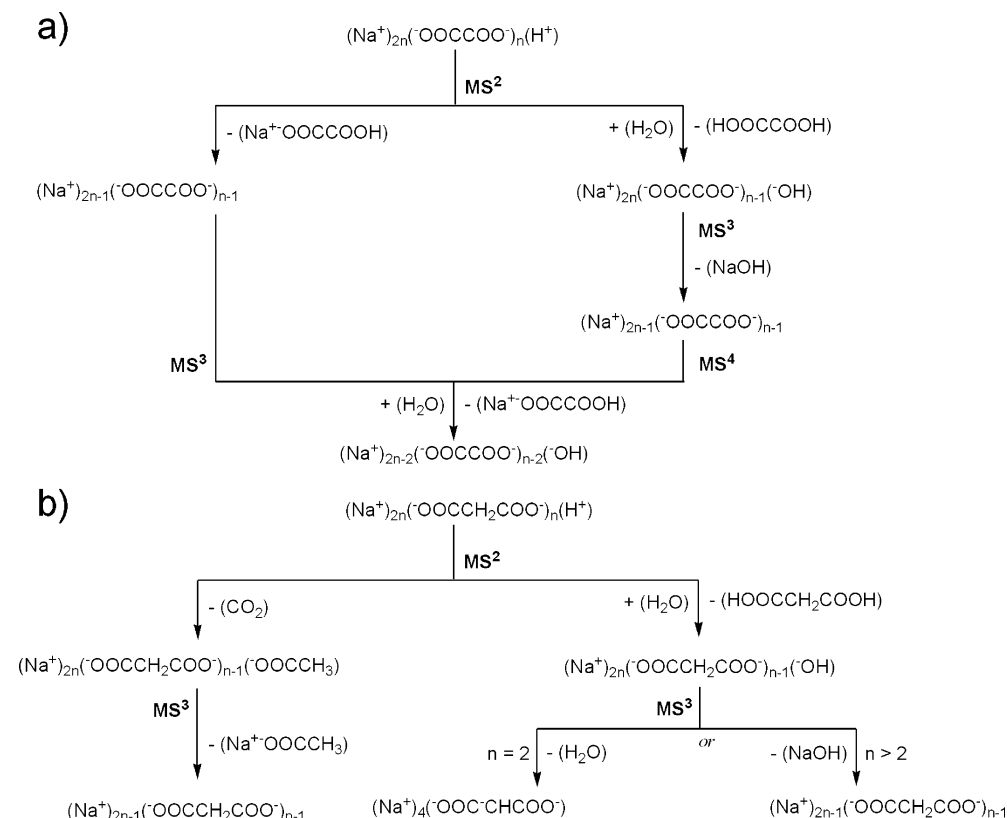
**Figure 5.** (a) CID spectrum of the proton-free sodiated malonate cluster,  $(\text{Na}^+)_3(\text{malonate}^{2-})_2$ , showing a major product resulting from decarboxylation with a water molecule attachment at  $m/z$  293 with a minor product yielded by the loss of sodium hydrogen malonate at  $m/z$  211. (b) MS<sup>3</sup> spectrum of the  $m/z$  293 product of MS<sup>2</sup>. (c) MS<sup>4</sup> spectrum of the  $m/z$  211 product of MS<sup>3</sup>.

products. Larger clusters ( $n = 3-6$ ) exhibit reactivity identical to that observed for the dimer.



**Figure 6.** (a) MS<sup>2</sup> spectrum of the sodiated hydrogen oxalate dimer,  $(\text{Na}^+)_4(-\text{OOC}\text{COO}^-)_2(\text{H}^+)$ , showing two competitive products at  $m/z$  157 and at  $m/z$  197. (b) MS<sup>3</sup> spectrum of the product at  $m/z$  197 showing the loss of sodium hydroxide ( $-40$  mass units). (c) CID of the product at  $m/z$  157 showing the exclusive product disodium hydroxide,  $(\text{Na}^+)_2(\text{OH}^-)$ , at  $m/z$  63.

An interesting dissociation of the cluster component via CID is observed from the products of proton-free malonate dimers.

**SCHEME 2: Reactions of Sodiated Hydrogen (a) Oxalate Clusters and (b) Malonate Clusters with Water Molecules Inferred from CID<sup>a</sup>**


<sup>a</sup> Indicated products are probed by MS<sup>3</sup> and MS<sup>4</sup>.

CID of the product at  $m/z$  211 yields two major products at  $m/z$  193 and  $m/z$  171 (Figure 5c). A minor product at  $m/z$  185 is also observed in the spectrum. The product at  $m/z$  193 results from the loss of the water ( $-18$  mass units). The structure of the ion at  $m/z$  211 is  $(\text{Na}^+)_{4}(\text{OOC}^-\text{CH}_2\text{COO}^-)(\text{OH})$ . To allow for dehydration of the cluster ion  $(\text{Na}^+)_{4}(\text{OOC}^-\text{CH}_2\text{COO}^-)(\text{OH})$ , the hydroxide ion must abstract a proton from the  $\alpha$ -carbon in the cluster. The products at  $m/z$  171 and  $m/z$  185 result from the loss of NaOH and decarboxylation with the attachment of a water molecule ( $-44 + 18 = -26$  mass units), respectively. Water attachment to the ion at  $m/z$  211 is observed at  $m/z$  229. Reactions of sodiated malonate clusters with a water molecule are shown in Scheme 1b.

**3.1.4. Longer Dicarboxylic Acids (C4–C6).** Monomeric dissociation of cationic proton-free sodiated succinate clusters via CID was reported by Ren et al.<sup>17</sup> Previous studies of anionic clusters of succinate, glutarate, and adipate (C4–C6) generally showed the loss of  $(\text{Na}^+)_{2}(\text{dicarboxylate}^{2-})$  by collisional activation.<sup>4</sup> All proton-free cationic sodiated dicarboxylate clusters of C4–C6 show exclusive losses of monomeric units,  $(\text{Na}^+)_{2}(\text{dicarboxylate}^{2-})$ , via CID.

**3.2. Sodiated Hydrogen Dicarboxylate Clusters.** Significant abundances of singly charged sodiated hydrogen dicarboxylate clusters with the composition  $(\text{Na}^+)_{2n}(\text{dicarboxylate}^{2-})_n(\text{H}^+)$ , where  $n = 1-5$ , are observed with small dicarboxylic acids, C2–C4, as seen in Figure 1. However, no significant amount of sodiated hydrogen dicarboxylate clusters were observed with glutaric acid (C5) and adipic acid (C6) samples (Figure 2).

**3.2.1. Oxalic Acid (C3) and Malonic Acid (C4).** A series of singly charged sodiated hydrogen oxalate clusters are found at  $m/z$  269, 403, 537, 671, 805, and 939, which correspond to  $n = 2, 3, 4, 5, 6$ , and 7, respectively (Figure 1a). Figure 6 shows

the CID spectra of the dimer,  $(\text{Na}^+)_{4}(\text{OOC}^-\text{COO}^-)_2(\text{H}^+)$ . The product at  $m/z$  157, which is identical to proton-free sodiated oxalate monomer, results from the loss of sodium hydrogen oxalate ( $-112$  mass units) and the product at  $m/z$  197 resulting from the loss of neutral oxalic acid following attachment of a water molecule ( $-90 + 18 = -72$  mass units). MS<sup>3</sup> of the product at  $m/z$  197 results in the loss of sodium hydroxide ( $-40$  mass units). The suggested structure of the product at  $m/z$  197 is  $(\text{Na}^+)_{4}(\text{OOC}^-\text{COO}^-)(\text{OH})$ . Reactions similar to those observed for the dimer characterize larger clusters ( $n = 3-4$ ) as well. However, the dimer shows the smallest relative intensity of the product resulting from the dissociation of sodium hydrogen oxalate ( $-112$  mass units) compared to the intensity of the product resulting from the dissociation of neutral oxalic acid via interaction with a water molecule ( $-72$  mass units). Reactions of sodiated hydrogen oxalate clusters are shown in Scheme 2a.

A series of singly charged sodiated hydrogen malonate clusters are found at  $m/z$  149, 297, 445, 593, 741, and 889 that correspond to  $n = 1, 2, 3, 4, 5$ , and 6, respectively (Figure 1b). Figure 7 shows the CID spectra of the dimer,  $(\text{Na}^+)_{4}(\text{OOC}^-\text{CH}_2\text{COO}^-)_2(\text{H}^+)$ . Isolation of the dimer peak followed by CID yields two distinct products at  $m/z$  253 and  $m/z$  211 (Figure 7a). The product at  $m/z$  253 results from decarboxylation ( $-44$  mass units). Loss of neutral malonic acid followed by the addition of a water molecule ( $-104 + 18 = -86$  mass units) yields the product at  $m/z$  211. The products were probed by MS<sup>3</sup>. MS<sup>3</sup> of the product at  $m/z$  253 shows exclusive loss of sodium acetate ( $\text{CH}_3\text{CO}_2\text{Na}$ ; 82 mass units). MS<sup>3</sup> of the product at  $m/z$  211 results in the same product as observed above in section 3.1.3. MS<sup>3</sup> of the product at  $m/z$  211 yields the product at  $m/z$  171 from the loss of sodium hydroxide ( $-40$  mass units;

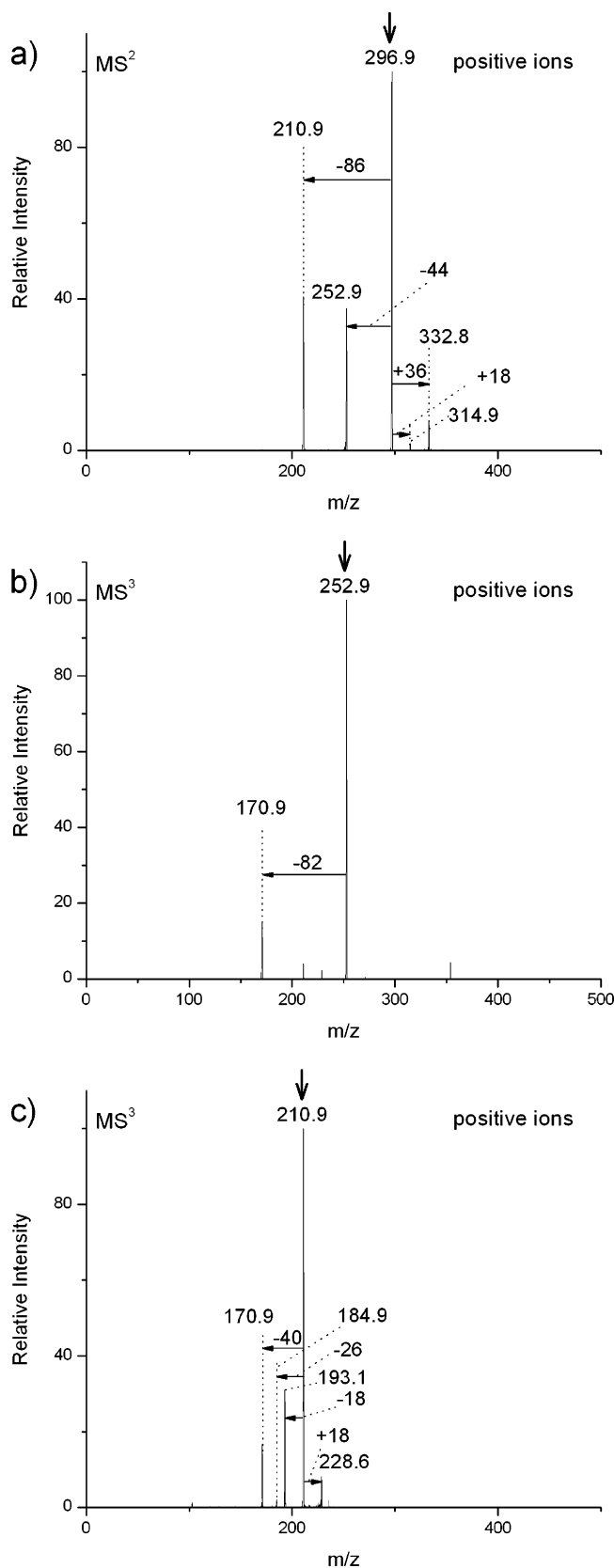


**Figure 7.** (a) CID spectrum of the sodium hydrogen malonate dimer, (Na<sup>+</sup>)<sub>4</sub>(-OOCCH<sub>2</sub>COO<sup>-</sup>)<sub>2</sub>(H<sup>+</sup>), showing two distinct products at *m/z* 253 and *m/z* 211. Two minor products are observed at *m/z* 315 and *m/z* 333. (b) CID of the product at *m/z* 253 showing the exclusive product at *m/z* 171. (c) MS<sup>3</sup> spectrum of the product at *m/z* 211 showing products at *m/z* 171 and at *m/z* 193. In addition, two minor products are observed at *m/z* 185 and at *m/z* 229.

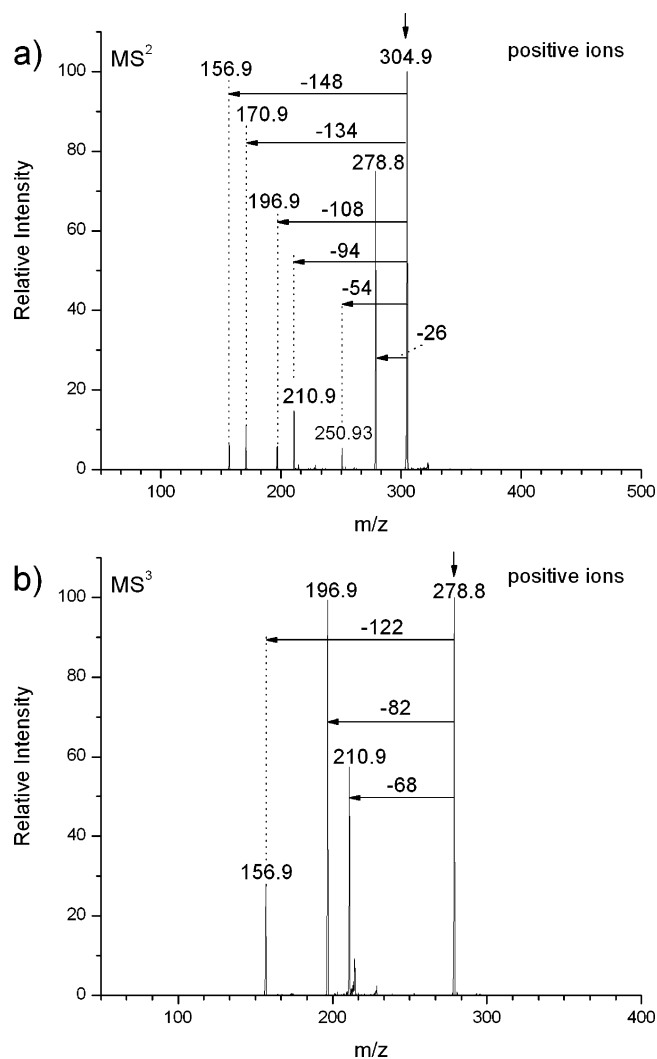


**Figure 8.** (a) CID spectrum of the mixed sodiated oxalate malonate dimer, (Na<sup>+</sup>)<sub>5</sub>(oxalate<sup>2-</sup>)(malonate<sup>2-</sup>), showing a major product at *m/z* 279. Minor products are observed at *m/z* 251, *m/z* 211, *m/z* 197, *m/z* 171, and *m/z* 157. (b) MS<sup>3</sup> spectrum of the product at *m/z* 279 showing three products at *m/z* 211, *m/z* 197, and *m/z* 157.

Figure 7c). In addition, a competitive dehydration product (-18 mass units) is also observed in the MS<sup>3</sup> spectrum of the product at *m/z* 211, again as noted above in section 3.1.3. Reactions of sodiated hydrogen malonate clusters are summarized in Scheme 2b.

Unlike proton-free sodiated oxalate clusters, decarboxylation of the oxalate anion in the sodiated hydrogen oxalate clusters is not observed (Figure 6a). In addition, sodiated hydrogen malonate clusters decarboxylate without concomitant water attachment as one of the competitive processes (Figure 7a). However, decarboxylation with water attachment is the exclusive CID process with proton-free malonate clusters (Figure 5a). The absence of decarboxylation of sodiated hydrogen oxalate clusters and the competitive decarboxylation of sodiated hydrogen malonate clusters without concomitant water attachment indicate the important role of a water molecule as a proton donor in the proton-free clusters.

**3.2.2. Succinic Acid (C4).** A series of singly charged sodiated hydrogen succinate clusters are found at *m/z* 163, 325, 487, 649, and 811, which correspond to *n* = 1, 2, 3, 4, and 5, respectively (Figure 1c). The CID spectrum of the dimer, (Na<sup>+</sup>)<sub>4</sub>(-OOCCH<sub>2</sub>-CH<sub>2</sub>COO<sup>-</sup>)<sub>2</sub>(H<sup>+</sup>), shows an exclusive product resulting from the loss of neutral succinic acid molecule following attachment

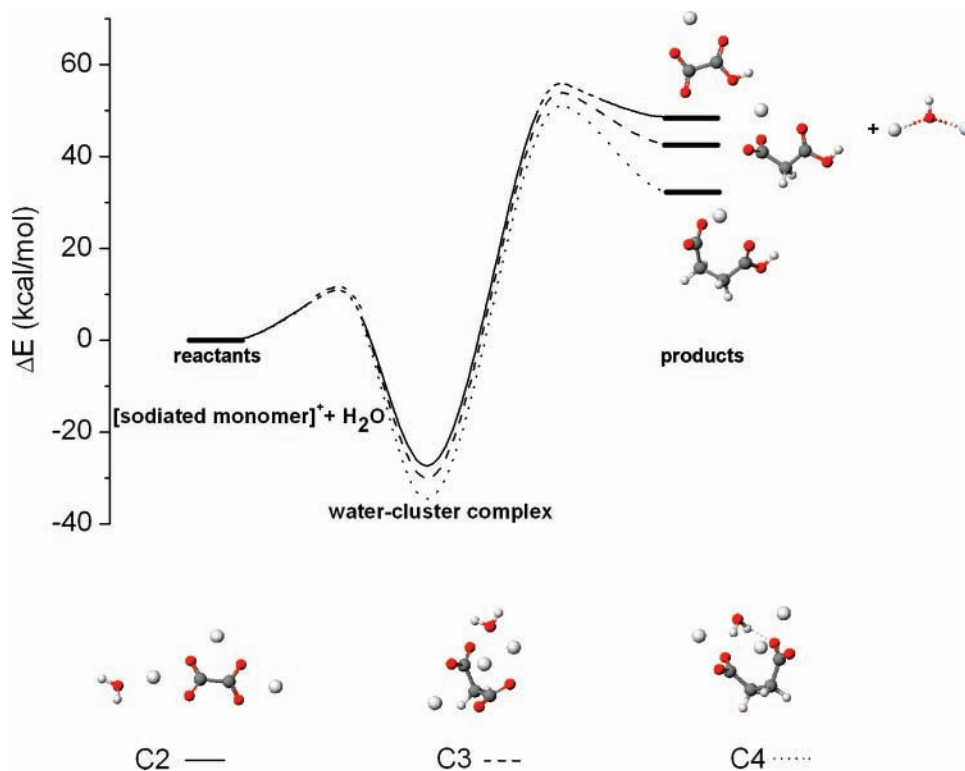


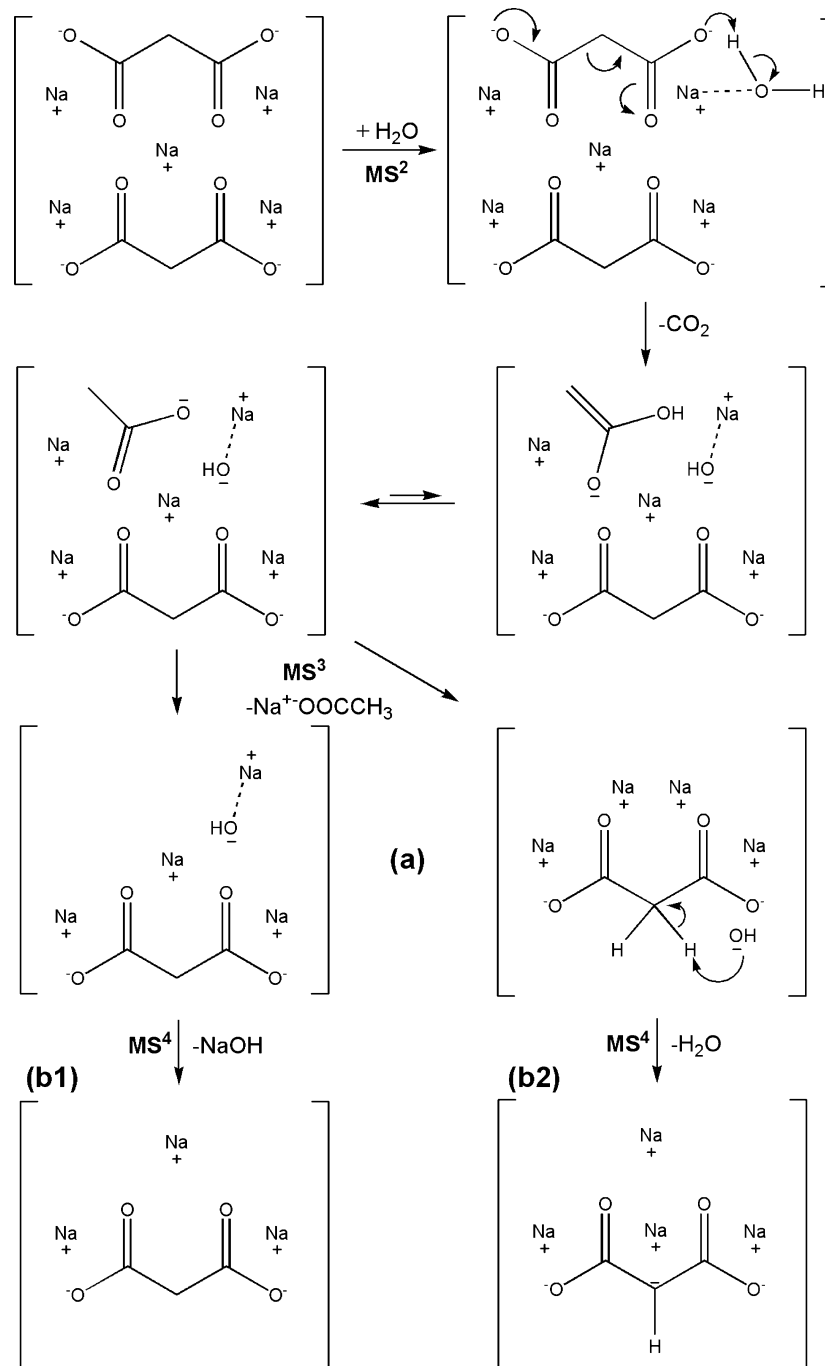
**Figure 9.** Reaction coordinate diagram showing relative energies in kilocalories per mole for cluster phase reactions of the sodiated dicarboxylate (C2–C4) monomers with a water molecule at the B3LYP/6-311G\*\* level, including zero-point correction obtained at the same scaled level. Barrier heights are not known. Optimized structures of the products and water complexes of sodiated oxalate (C2) monomer, sodiated malonate (C3) monomer, and sodiated succinate (C4) monomer are shown in the diagram and below the diagram, respectively. The hydrogen bond is indicated with dashed lines.

of a water molecule ( $-118 + 18 = -100$  mass units). The water molecule donates a proton to the singly charged succinate ion ( $\text{HOOCCH}_2\text{CH}_2\text{COO}^-$ ) with a hydroxide ion remaining in the cluster. This is confirmed by the  $\text{MS}^3$  spectrum of the product, which shows the loss of sodium hydroxide ( $-40$  mass units). Two distinct products are observed in the CID spectrum of the trimer,  $(\text{Na}^+)_6(\text{OOCCH}_2\text{CH}_2\text{COO}^-)_3(\text{H}^+)$ , at  $m/z$  387 and  $m/z$  347. The loss of neutral succinic acid molecule following attachment of a water molecule yields the product at  $m/z$  387. The product at  $m/z$  347 results from the loss of sodium hydrogen succinate ( $-140$  mass units). The CID of the tetramer,  $(\text{Na}^+)_8(\text{OOCCH}_2\text{CH}_2\text{COO}^-)_4(\text{H}^+)$ , yields one major product at  $m/z$  509 by the loss of sodium hydrogen succinate. The pentamer at  $m/z$  811 in Figure 1c exhibits CID pathways similar to the tetramer.

**3.3. Sodiated Mixed Dicarboxylate Clusters.** The smaller diacids, especially oxalic and malonic acids, exhibit the most interesting cluster reactions, many of which involve the cleavage of C–C bonds. As a result we decided to compare the reactivity of different diacids when they are present in the same cluster. To accomplish this, mixtures of the sodium dicarboxylic acids were prepared and investigated. A series of singly charged sodiated mixed dicarboxylate clusters,  $(\text{Na}^+)_{2n+1}(\text{oxalate}^{2-})_a(\text{dicarboxylate}^{2-})_b$ , where  $a + b = n$  and  $n = 1-4$ , are found where the dicarboxylate is malonate or succinate from mixtures of oxalic acid with other dicarboxylic acids (C3–C6). The mixtures of oxalic acid with glutaric acid or adipic acid show a major peak at the sodiated glutarate monomer or sodiated adipate monomer, respectively. In mixtures with malonic acid, a series of singly charged sodiated hetero dicarboxylate clusters,  $(\text{Na}^+)_{2n+1}(\text{malonate}^{2-})_a(\text{dicarboxylate}^{2-})_b$ , where  $a + b = n$  and  $n = 1-4$ , are observed with all of the other dicarboxylic acids (C2, C4–C6). The  $\text{MS}^2$  spectra of

sodiated oxalate succinate clusters exhibit  $\text{MS}^2$  spectra similar to proton-free sodiated oxalate clusters, which are characterized by the losses of 26, 54, and 94 mass units along with monomeric dissociation, as seen in Figure 4b.  $\text{MS}^3$  spectra of the corresponding products confirm that water molecules interacting with the collisionally activated clusters react exclusively with oxalate anions in the clusters. The CID spectra of the sodiated mixed dicarboxylate clusters of malonic acid show a single product, resulting from the elimination of  $\text{CO}_2$  with the attachment of a  $\text{H}_2\text{O}$  molecule ( $-44 + 18 = -26$  mass units).  $\text{MS}^3$  spectra confirm that the reactions with water molecules have occurred only with malonate anions in the clusters.

The CID spectra of the sodiated oxalate malonate dimer,  $(\text{Na}^+)_5(\text{oxalate}^{2-})(\text{malonate}^{2-})$ , are shown in Figure 8. CID of the dimer cluster at  $m/z$  305 yields a major product at  $m/z$  279, resulting from the elimination of  $\text{CO}_2$  with the attachment of a  $\text{H}_2\text{O}$  molecule (Figure 8a). Minor products are observed at  $m/z$  251, 211, 197, 171, and 157. These minor products correspond to products observed for the reactions of proton-free sodiated oxalate clusters ( $m/z$  251 and  $m/z$  211) with water molecules and monomeric dissociation of sodiated oxalate ( $m/z$  171) or sodiated malonate ( $m/z$  157). The product at  $m/z$  197 results from the elimination of sodium hydrogen malonate following the attachment of a water molecule ( $-126 + 18 = -108$  mass units). The  $\text{MS}^3$  spectrum of the product at  $m/z$  279 shows that the product results from the reactions of an oxalate anion or a malonate anion with a water molecule in the clusters (Figure 8b). The product at  $m/z$  211, resulting from the elimination of sodium formate ( $\text{HCO}_2\text{Na}$ , 68 mass units), confirms that the product at  $m/z$  279 in the  $\text{MS}^2$  spectrum results from the reaction of the oxalate anion with a water molecule. The product at  $m/z$  197 results from the elimination of sodium acetate ( $\text{NaO}_2\text{C}_2\text{H}_3$ , 82 mass units), and the product at  $m/z$  157 is formed by

SCHEME 3: Proposed Reaction Mechanisms of Sodiated Malonate Dimer with a Water Molecule<sup>a</sup>

<sup>a</sup> Optimized geometries and energy changes for corresponding labeled states are shown in Figure 10.

the elimination of sodium acetate with sodium hydroxide ( $-82-40 = -122$  mass units). These two products suggest that the product at  $m/z$  279 in the MS<sup>2</sup> spectrum also results from the reaction of the malonate anion with a water molecule. The products resulting from the reactions of a water molecule with the malonate anion are only 1.2 times more abundant than the products of reaction with the oxalate anion. The decarboxylation product resulting from the reaction of malonate with water has approximately twice the abundance when compared to the similar reaction of oxalate with water. The relative product yields imply the majority of the decarboxylation products result from the reaction of malonate with water rather than the reaction of oxalate with water in the mixed cluster.

**3.4. Theoretical Results.** To probe the mechanisms and energetics of the observed cluster phase reactions, the optimized

geometries of the ground-state reactants and products of cationic small dicarboxylate (C<sub>2</sub>–C<sub>6</sub>) clusters and corresponding electronic energies have been investigated through the computational methods described in section 2.

**3.4.1. Sodiated Dicarboxylate Monomers.** As discussed in section 3.1.1, the elimination of the sodium hydrogen dicarboxylate via single water molecule attachment to yield (Na<sup>+</sup>)<sub>2</sub>(<sup>-</sup>OH) is observed as a facile reaction for the three smallest dicarboxylate monomers. Calculated changes of electronic energy ( $\Delta E$ ) for the reactions of sodiated C<sub>2</sub>–C<sub>4</sub> monomers with water molecules are shown in Figure 9 with DFT optimized geometries of the products and the monomer–water complexes. It is notable that the energy stabilization via formation of the monomer–water complex is enhanced from C<sub>2</sub> to C<sub>4</sub>. DFT optimized geometries of the monomer–water

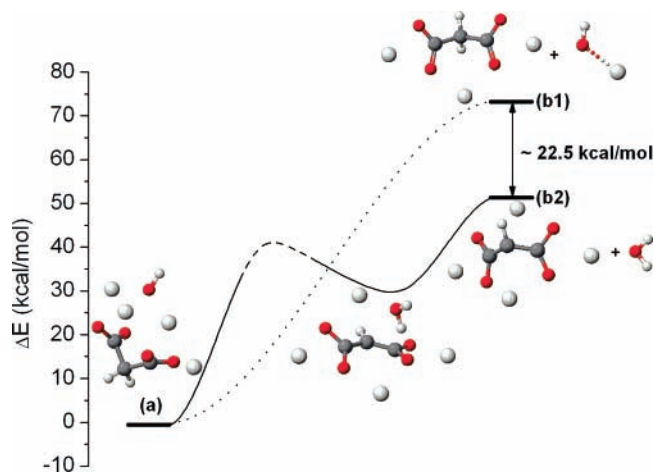


**Figure 10.** Reaction coordinate diagram showing relative energies in kilocalories per mole for MS<sup>4</sup> of the proton-free sodiated malonate dimer at the B3LYP/6-311G\*\* level, including zero-point correction at the same scaled level. The reactant results from decarboxylation of malonate anion with a water molecule attachment followed by the elimination of sodium acetate through MS<sup>2</sup> and MS<sup>3</sup> of proton-free sodiated malonate dimer. Barrier heights are not known. Optimized geometries for corresponding states are obtained at the same scaled level. The reaction mechanisms are shown in Scheme 3.

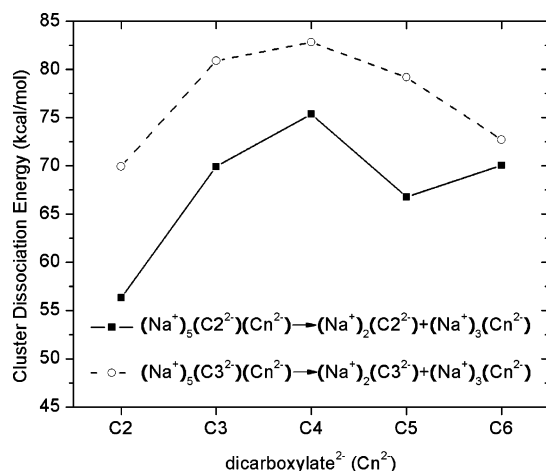


**Figure 11.** Plots of calculated cluster dissociation energies of the proton-free sodiated mixed dicarboxylate dimers with oxalic acid (C2) or malonic acid (C3) versus the number of dicarboxylic acid carbons. The cluster dissociation energy is determined by the energy difference between the total electronic energy of the separated species of the neutral disodiated C2 or C3 and the trisodiated monomeric cation of larger dicarboxylate and the electronic energy of the cluster.

complexes show that the interaction between sodiated dicarboxylate monomers and water increases from C2 to C4.

**3.4.2. Proton-Free Sodiated Dicarboxylate Clusters.** Not surprisingly, DFT optimized geometries of the clusters show that oxygen atoms of doubly deprotonated dicarboxylate anions interact strongly with sodium cations in the clusters. In the present and prior<sup>4</sup> investigations, we have shown that water molecules donate protons to dicarboxylate anions, which initiate chemical processes including decarboxylation of the diacids. MS<sup>n</sup> spectra of the malonate dimer have shown that, in this reaction, the hydroxide ion abstracts a proton from the  $\alpha$ -carbon of the malonate ion in the product cluster ion (Na<sup>+</sup>)<sub>4</sub>(<sup>-</sup>OOCCH<sub>2</sub>COO<sup>-</sup>)(<sup>-</sup>OH) (Figure 5c). Calculated  $\Delta E$  through MS<sup>4</sup> of the malonate dimer via decarboxylation of the diacid is shown in Figure 10. As seen in Figure 10, the reaction process, in which a water molecule leaves the clusters after the hydroxide ion abstracts a proton from the  $\alpha$ -carbon of the

malonate ion, is energetically favored by  $\sim 22.5$  kcal/mol. This reaction process is favored because the deprotonation of the acidic  $\alpha$ -carbon of the malonate anion, C<sub>3</sub>HO<sub>4</sub><sup>3-</sup>, is favored by the resulting charge delocalization. Of note, only the dimer shows the elimination of water from the product, while larger clusters show the exclusive loss of NaOH. The proposed reaction mechanisms between a sodiated malonate dimer and a water molecule are shown in Scheme 3.

**3.4.3. Sodiated Mixed Dicarboxylate Clusters.** The DFT calculated cluster dissociation energies of the mixed dicarboxylate dimers of oxalate or malonate are shown in Figure 11. The cluster dissociation energies are the differences of the total electronic energy of the separated species of the neutral disodiated C2 or C3 and the cationic trisodiated dicarboxylate and the electronic energy of the cluster. The mixed dicarboxylate clusters with a malonate anion are bound more strongly than the corresponding mixed dicarboxylate clusters with an oxalate anion. The optimized geometries of sodiated mixed dicarboxylate clusters show that carboxylate groups of anions are facing to the center of the cluster interacting with sodium cations, with the exception of the rigid oxalate anion. The distances between an oxygen atom of a carboxylate group to the neighbored oxygen atom of the other carboxylate group are in the range of 3.2–3.7 Å in the dimeric clusters. The corresponding distance in the case of oxalate anion involves the shorter distance of 2.75 Å, with a relatively planar structure. In the mixed dicarboxylate dimers with malonate anion, the distances between an oxygen atom of a carboxylate group to the neighboring oxygen atom of a carboxylate group of larger dicarboxylate anions are longer, by 0.1 (succinate) to 0.5 Å (adipate) when compared to their own homodimers. However, the distance increases by 0.5 (malonate) to 2.5 Å (adipate) in the mixed dimers with oxalate anion. It is inferred that these differences in the structures of larger dicarboxylate anions weaken the interactions between sodium cations and carboxylate groups in the dimeric clusters with oxalate ion. As discussed in section 3.3, cluster phase reactions with water molecules are observed with all mixed dicarboxylate dimers with a malonate anion. However, among sodiated mixed dicarboxylate dimers of the oxalate anion, only the oxalate malonate dimer and the oxalate succinate dimer exhibit complex cluster phase reactions. On the basis of the observed reactions of the clusters, it generally appears that a cluster dissociation energy greater than  $\sim 70$  kcal/mol serves to facilitate the cluster phase reactions (Figure 11).

Through the observation of the reactions of small sodiated dicarboxylate clusters in the present study, we note that oxalate anions and malonate anions almost always react with water molecules. As discussed in section 3.3, the relative intensity of the products show that there is approximately twice as much product resulting from the reaction of the malonate anion with a water molecule in the product at *m/z* 279 (Figure 8b). The calculated  $\Delta E$  of the reactions of a sodiated oxalate malonate dimer with a water molecule are shown in Figure 12, along with the optimized geometries of the corresponding intermediates. In the water–cluster complex, the oxygen atom of the water molecule interacts with a sodium cation, while a hydrogen atom is bound to a carboxylate oxygen in oxalate or malonate. The water–cluster complex, in which the water molecule interacts with the oxalate anion, is  $\sim 3$  kcal/mol lower than with the malonate anion. The reaction intermediate, in which the proton is transferred from water to oxalate anion, is  $\sim 5.7$  kcal/mol lower than the corresponding reaction intermediate of the protonated malonate anion in the cluster. Through the complexes and intermediate products shown in Figure 12, energetically

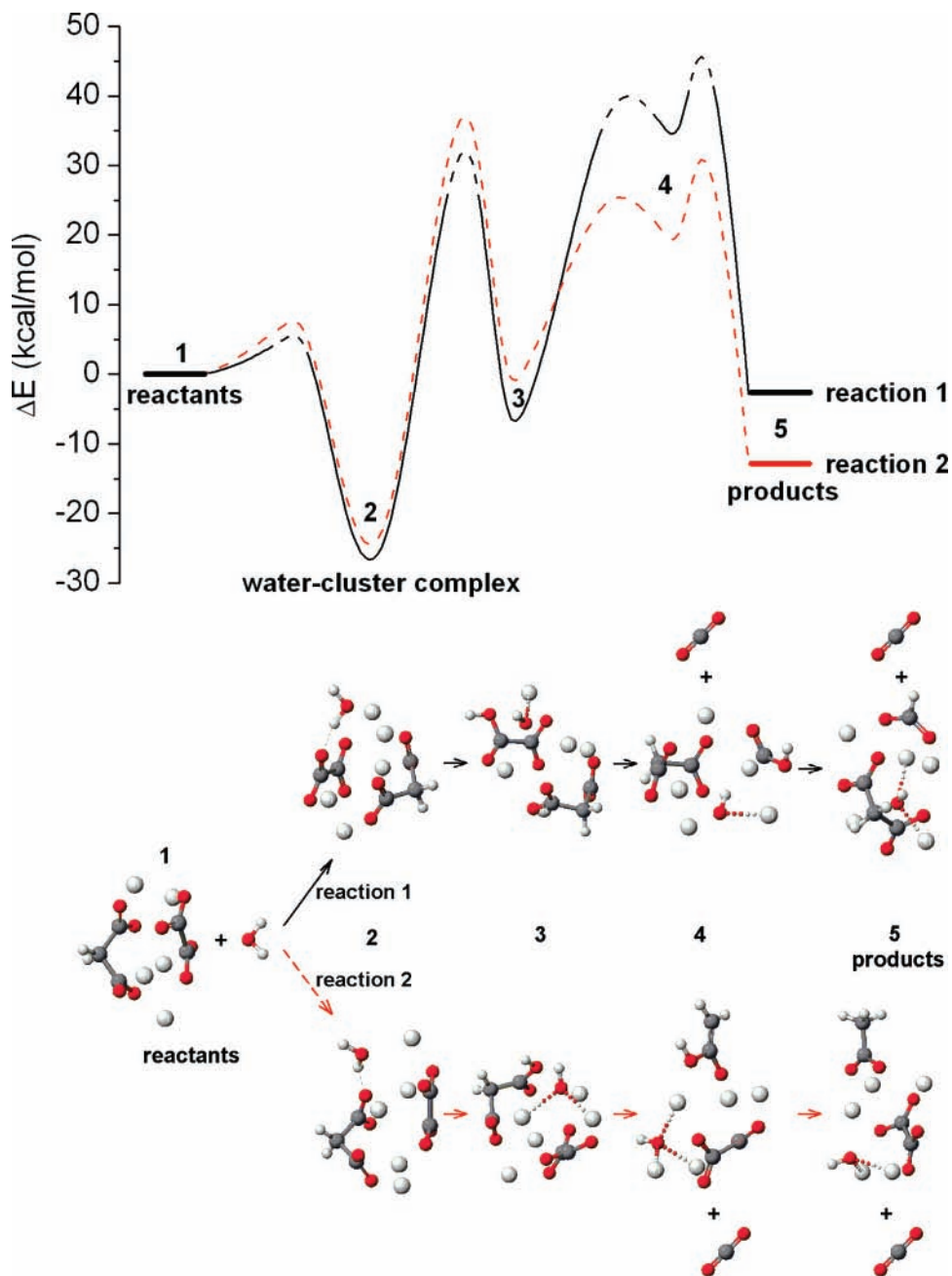


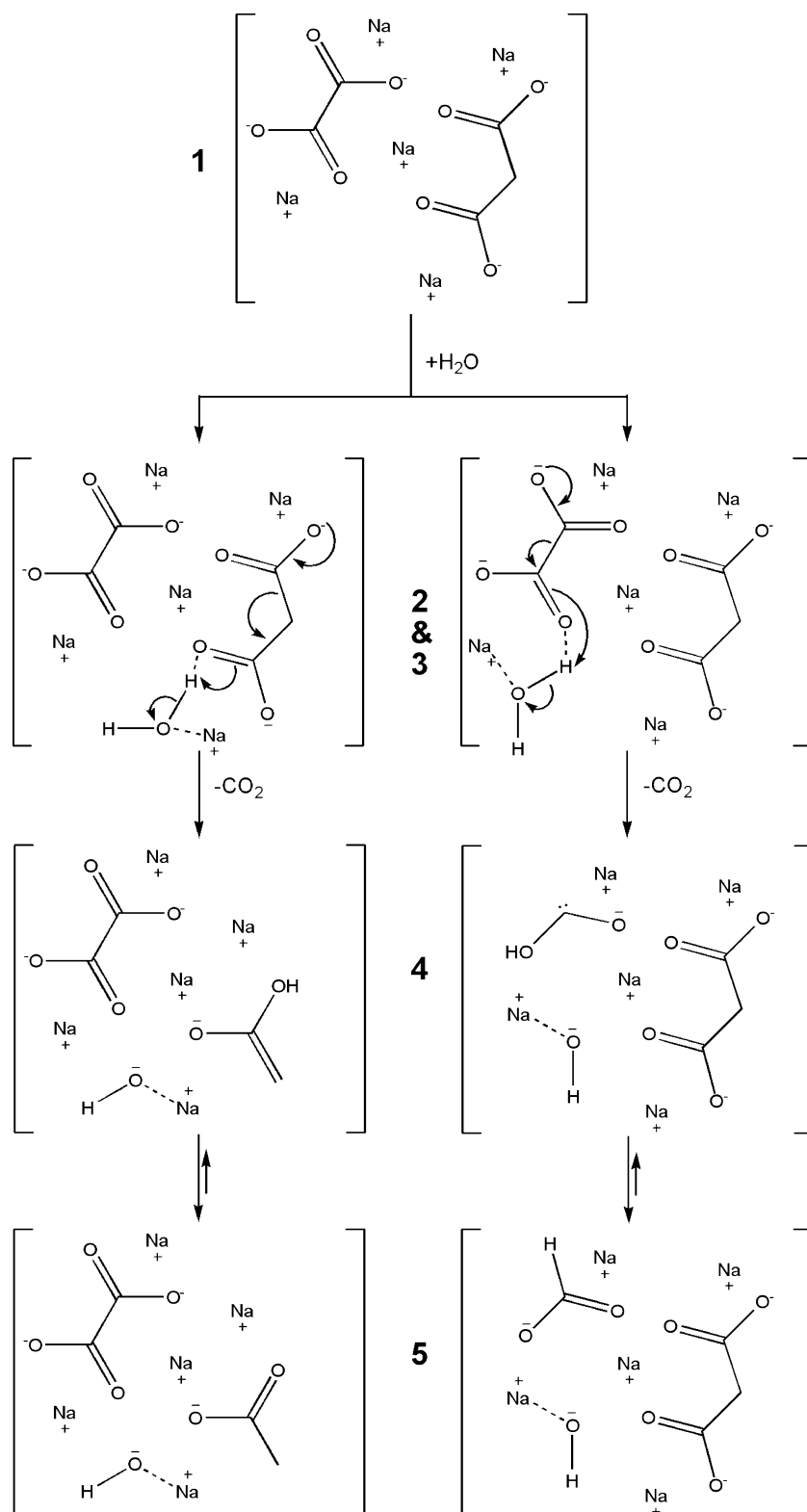
**Figure 12.** Reaction coordinate diagram showing relative energies in kilocalories per mole for cluster phase reactions of the sodiated oxalate malonate dimer,  $(\text{Na}^+)_5(\text{oxalate}^{2-})(\text{malonate}^{2-})$ , with a water molecule at the B3LYP/6-311G\*\* level, including zero-point correction obtained at the same scaled level. Decarboxylation of oxalate dianion following a water molecule attachment in the cluster is shown as reaction 1, while decarboxylation of malonate dianion following a water molecule attachment is shown as reaction 2. Barrier heights are not known. Optimized geometries for corresponding states are obtained at the same scaled level. The reaction mechanism of each numbered step is shown in Scheme 4.

unstable dihydroxycarbene anion products (reaction 1) or enol acetate products (reaction 2) are expected to form with a hydroxide ion in the cluster after decarboxylation of malonate or oxalate, respectively. The rearrangements of the unstable  $\text{HOCO}^-$  (reaction 1) and  $\text{HOOCCH}_2^-$  (reaction 2) to formate ( $^- \text{OOCH}$ ) and acetate ( $^- \text{OOCCH}_3$ ) are expected since these transformations lower the energies of the cluster by  $\sim 38$  and  $\sim 35$  kcal/mol, respectively. The energy of the product resulting from the decarboxylation of malonate anion in the cluster is  $\sim 10$  kcal/mol lower than the energy of the product from decarboxylation of oxalate anion. It is inferred that formation of electronically conjugated  $\text{HOOCCH}_2^-$  from decarboxylation of malonate ion is more energetically favored than formation of  $\text{HOCO}^-$  from oxalate ion. Further, theoretical studies of the activation barrier for the formation of formic acid from

decarboxylation of oxalic acid through dihydroxycarbene intermediates requires approximately 70 kcal/mol.<sup>18</sup> It is likely that the strained transition state for hydrogen migration from oxygen to carbon is responsible for the high activation barrier. As a result, decarboxylation of the malonate anion in the cluster, which is initiated by donation of a proton from a water molecule to malonate anion, is more likely to occur (Figure 8b). Proposed mechanisms of the observed decarboxylation reactions of the sodiated oxalate malonate dimer are shown in Scheme 4

#### 4. Conclusion

Collisionally activated cationic clusters of small dicarboxylate anions with sodium cations undergo reactions with water molecules in the gas phase. In contrast to anionic sodiated

SCHEME 4: Proposed Reaction Mechanisms of Sodiated Oxalate Malonate Dimer with a Water Molecule<sup>a</sup>

<sup>a</sup> Optimized geometries and energy changes for corresponding numbered states are shown in Figure 12.

dicarboxylate clusters, significant abundances of singly charged sodiated dicarboxylate monomers,  $(\text{Na}^+)_3(\text{dicarboxylate}^{2-})$ , and sodiated hydrogen dicarboxylate clusters,  $(\text{Na}^+)_{2n}(\text{dicarboxylate}^{2-})_n(\text{H}^+)$ , where  $n = 1-6$ , are observed along with their reactions with water molecules. Similar to what is observed with anionic clusters, cationic clusters of longer dicarboxylate ions (C4–C6) generally exhibit sequential loss of disodium dicarboxylate moieties, while collisionally activated oxalate (C2) and

malonate (C3) clusters generally exhibit chemical reactions with water molecules. Water molecules donate protons to dicarboxylate anions, initiating chemical processes including decarboxylation of the diacid. Decarboxylation with water attachment is a major and dominating reaction of proton-free sodiated C2 and C3 clusters, respectively. However, decarboxylation is not the dominant reaction with sodiated hydrogen C3 clusters, and it is not observed with sodiated hydrogen C2 clusters. Dehydration

from the product of the C3 dimer is observed and analyzed as a favored dissociation pathway. The hydroxide ion in the cluster can pick up a proton from the  $\alpha$ -carbon due to the energetically favored delocalization of the triply deprotonated malonate anion. Studies of competitive reactivity of different mixed dicarboxylate clusters demonstrate that malonate anion readily undergoes decarboxylation in preference to oxalate anion via interaction with a water molecule when both are present in a cluster. This difference is mainly attributed to the more stable products resulting from the reaction of malonate ion with a water molecule.

**Acknowledgment.** The research described in this paper was carried out at the Beckman Institute and the Noyes Laboratory of Chemical Physics at the California Institute of Technology. We appreciate the support provided by the Mass Spectrometry Resource Center, Materials and Process Simulation Center in the Beckman Institute, and Planetary Science & Life Detection section, Jet Propulsion Laboratory, California Institute of Technology. Partial support was also provided by the National Science Foundation (NSF) under Grant No. CHE-0416381.

### References and Notes

(1) Julian, R. R.; Beauchamp, J. L. *Int. J. Mass Spectrom.* **2003**, *227*, 147.

- (2) Hodyss, R.; Cox, H. A.; Beauchamp, J. L. *J. Phys. Chem. A* **2004**, *108*, 10030.
- (3) Cox, H. A.; Hodyss, R.; Beauchamp, J. L. *J. Am. Chem. Soc.* **2005**, *127*, 4084.
- (4) Kim, H. I.; Goddard, W. A.; Beauchamp, J. L. *J. Phys. Chem. A* **2006**, *110*, 7777.
- (5) Vollhardt, K. P.; Schore, N. E. *Organic Chemistry: Structure and Function*, 3rd ed.; W. H. Freeman and Company: New York, 1999.
- (6) Kawamura, K.; Usukura, K. *J. Oceanog.* **1993**, *49*, 271.
- (7) Sempere, R.; Kawamura, K. *Global Biogeochem. Cycles* **2003**, *17*.
- (8) Crahan, K. K.; Hegg, D.; Covert, D. S.; Jonsson, H. *Atmos. Environ.* **2004**, *38*, 3757.
- (9) Gao, S.; Keywood, M.; Ng, N. L.; Surratt, J.; Varutbangkul, V.; Bahreini, R.; Flagan, R. C.; Seinfeld, J. H. *J. Phys. Chem. A* **2004**, *108*, 10147.
- (10) Baboukas, E. D.; Kanakidou, M.; Mihalopoulos, N. *J. Geophys. Res., [Atmos.]* **2000**, *105*, 14459.
- (11) Myhre, C. E. L.; Nielsen, C. J. *Atmos. Chem. Phys.* **2004**, *4*, 1759.
- (12) Gard, E. E.; Kleeman, M. J.; Gross, D. S.; Hughes, L. S.; Allen, J. O.; Morrical, B. D.; Fergenson, D. P.; Dienes, T.; Galli, M. E.; Johnson, R. J.; Cass, G. R.; Prather, K. A. *Science* **1998**, *279*, 1184.
- (13) Woodcock, A. H. *J. Meteor.* **1953**, *10*, 362.
- (14) Becke, A. D. *J. Chem. Phys.* **1993**, *98*, 5648.
- (15) Lee, C. T.; Yang, W. T.; Parr, R. G. *Phys. Rev. B* **1988**, *37*, 785.
- (16) Harihara, P.; Pople, J. A. *Chem. Phys. Lett.* **1972**, *16*, 217.
- (17) Ren, D.; Polce, M. J.; Wesdemiotis, C. *Int. J. Mass Spectrom.* **2003**, *228*, 933.
- (18) Higgins, J.; Zhou, X. F.; Liu, R. F.; Huang, T. T. S. *J. Phys. Chem. A* **1997**, *101*, 2702.